HHS Public Access

Author manuscript

Sci Transl Med. Author manuscript; available in PMC 2019 September 28.

Published in final edited form as:

Sci Transl Med. 2017 October 04; 9(410): . doi:10.1126/scitranslmed.aal3693.

Rapid pathogen-specific phenotypic antibiotic susceptibility testing using digital LAMP quantification in clinical samples

Nathan G. Schoepp[1,*], **Travis S. Schlappi**[1,*], **Matthew S. Curtis**[1], **Slava S. Butkovich**[1], **Shelley Miller**[2], **Romney M. Humphries**[2], **Rustem F. Ismagilov**[1,†]

[1]Division of Chemistry and Chemical Engineering, California Institute of Technology, 1200 East California Boulevard, Pasadena, CA 91125, USA.

[2]Department of Pathology and Laboratory Medicine, University of California, Los Angeles, 10888 Le Conte Avenue, Brentwood Annex, Los Angeles, CA 90095, USA.

Abstract

Rapid antimicrobial susceptibility testing (AST) is urgently needed for informing treatment decisions and preventing the spread of antimicrobial resistance resulting from the misuse and overuse of antibiotics. To date, no phenotypic AST exists that can be performed within a single patient visit (30 min) directly from clinical samples. We show that AST results can be obtained by using digital nucleic acid quantification to measure the phenotypic response of *Escherichia coli* present within clinical urine samples exposed to an antibiotic for 15 min. We performed this rapid AST using our ultrafast (~7 min) digital real-time loop-mediated isothermal amplification (dLAMP) assay [area under the curve (AUC), 0.96] and compared the results to a commercial (~2 hours) digital polymerase chain reaction assay (AUC, 0.98). The rapid dLAMP assay can be used with SlipChip microfluidic devices to determine the phenotypic antibiotic susceptibility of *E. coli* directly from clinical urine samples in less than 30 min. With further development for additional

†Corresponding author. rustem.admin@caltech.edu.
*These authors contributed equally to this work.

Author contributions:

The order of co-first authors was determined by coin toss. T.S.S., N.G.S., and R.F.I. contributed to the design and/or interpretation of the reported experiments or results. T.S.S., N.G.S., M.S.C., S.S.B., and R.F.I. contributed to the acquisition and/or analysis of the data. T.S.S., N.G.S., R.M.H., and R.F.I. contributed to the drafting and/or revising of the manuscript. M.S.C. was primarily responsible for real-time imaging acquisition and analysis. S.M. and R.M.H. were primarily responsible for acquiring clinical samples and performing gold standard broth microdilution ASTs. R.F.I. and R.M.H. contributed administrative, technical, and supervisory support.

Competing interests:

R.F.I., T.S.S., M.S.C., and N.G.S. are inventors on a patent (PCT/US2015/059344) filed by Caltech and SlipChip Corp. and on provisional patent applications 62/399,196 and 62/460,625 filed by Caltech that cover devices and methods for rapid digital antibiotic susceptibility testing. R.F.I. has a financial interest in SlipChip Corp. and is a consultant for SlipChip Corp.

Data and materials availability:

Requests for additional information should be addressed to R.F.I. (rustem.admin@caltech.edu).

SUPPLEMENTARY MATERIALS

www.sciencetranslationalmedicine.org/cgi/content/full/9/410/eaal3693/DC1

Materials and Methods

Fig. S1. Resolution of digital devices.

Fig. S2. Real-time dLAMP DNA quantification of a UTI sample with nit treatment.

Fig. S3. The dAST method tested with isolates with near-intermediate MICs.

Fig. S4. Reproducibility of the dAST method with clinical urine samples.

Table S1. Concentration of clinical urine samples.

Table S2. Clinical samples used in this study.

Table S3. Rapid phenotypic AST literature summary showing the state of the art. References (88–101)

pathogens, antibiotics, and sample types, rapid digital AST (dAST) could enable rapid clinical decision-making, improve management of infectious diseases, and facilitate antimicrobial stewardship.

INTRODUCTION

The emergence of antibiotic resistance is an impending threat to global health. It is projected to cause 10 million deaths and more than $1 trillion in total economic impact by 2050 if left unchecked (1, 2). To combat antimicrobial resistance, facilitate stewardship, and improve patient outcomes, health care providers need to be able to determine antibiotic susceptibility rapidly and ideally at the point of care (POC) (3–6). The need for rapid antimicrobial susceptibility testing (AST) to guide antibiotic treatment is recognized by all major health organizations, including the Centers for Disease Control and Prevention and the World Health Organization (7–11).

Urinary tract infections (UTIs) are among the most common bacterial infections, accounting for ~8 million primary care visits annually, and are almost always treated with antibiotics (12, 13). In the absence of a rapid AST, UTIs are among the many infections that are treated with second-line antibiotics, such as the fluoroquinolone ciprofloxacin (dp), instead of first-line antibiotics, such as nitrofurantoin (nit) (14). This increased use of fluoroquinolones is accompanied by the emergence of fluoroquinolone resistance, limiting treatment options, which is especially critical in life-threatening cases, such as when UTIs progress to sepsis. Thus, UTIs are a specific clinical scenario where an inexpensive and rapid (within the ~30-min duration of a patient visit) AST would notably improve patient outcomes and antimicrobial stewardship.

No such AST diagnostic currently exists. Phenotypic AST methods based on culture of the target pathogen are the current gold standard but are too slow to support immediate treatment decisions or to be implemented at the POC (15). Genotypic methods, which detect known resistance genes, are faster because they do not require a culturing step (16–18). Genotypic methods have shown promise in select clinical settings where the presence of a single gene yields high predictive value, such as testing for mecA to detect methicillin-resistant *Staphylococcus aureus* (19–21). However, genotypic tests have not been implemented more broadly because they are not generalizable to different pathogens or mechanisms of resistance, especially in the case of Gram-negative bacteria, for which more than 800 resistance genes are known for b-lactam class antibiotics alone (22).

An ideal AST would test the phenotypic response of a pathogen to antibiotics in a pathogen-specific manner and provide an AST answer (susceptible or resistant) in less than 30 min (23,24). This is a critical bar to meet because if the AST result can be obtained within the time span of a patient visit, then the information can be used to inform treatment and facilitate antimicrobial stewardship at the POC. Additionally, in some infections, such as sepsis, accelerated time to treatment is correlated with improved patient outcome (25). To achieve this speed, the AST method needs to work directly from a clinical sample. Several methods, including our previous work (26), have improved the speed of individual steps of the phenotypic AST workflow (such as pathogen isolation and identification, antibiotic

exposure time, sample preparation, and readout), but few of these papers report performing the entire workflow from start to finish using a clinical sample.

To date, no phenotypic AST has achieved a sample-to-answer result in less than 30 min directly from a clinical sample. Most of the methods under development were validated with clinical isolates of pathogens, which before the assay were grown in culture to a high density and not directly with clinical samples. Among the rapid phenotypic AST methods used with clinical samples, one microscopy-based method could differentiate susceptible and resistant isolates after only 10 min of antibiotic exposure but did not test clinical samples (27). A similarly rapid microscopy-based method could detect differences in bacterial growth during antibiotic treatment after as short as 6 min of antibiotic exposure using isolates, but the total assay time for a clinical sample was 155 min (28). As discussed in (28), clinical sample matrices, such as urine, present a challenge for rapid microscopy-based ASTs, affecting the speed and sensitivities (required cell concentrations) of these assays.

Furthermore, identification and differentiation of target pathogens from commensal organisms can be challenging if these steps rely only on imaging, without the molecular specificity offered by other methods. A microfluidic-based microscopy method using isolates reported AST in ~3 to 4 hours without an identification step and estimated that the total assay time from a clinical sample would be 52 hours (29). Another microscopy-based method in clinical testing performs identification and AST from a positive culture in 5 to 6 hours, with additional overnight or longer time required to first grow the culture from a clinical sample (30, 31). An electrochemical method was used to determine susceptibility in as short as 25 min using nonspecific redox markers for reference strains (32), but the workflow lacked a pathogen identification step and the AST was not pathogen-specific. Other electrochemical methods are pathogen-specific but require at least 45 min of assay time when using isolates (33). Pathogen-specific electrochemical methods have also been used to determine susceptibility from clinical samples, but assay times were on the order of hours (34). Methods that perform phenotypic AST by quantifying nucleic acids (NAs) are promising because they provide molecular specificity, but so far, most have required long antibiotic exposures (~2 hours or more) in addition to the time required for measurement, which was as fast as 1.5 hours using isothermal amplification (35–37). This promise of an NA-based AST was highlighted in a study that used RNA gene expression markers and demonstrated antibiotic exposure times as short as 10 min for isolates and as short as 30 min for clinical samples, although in that landmark study, the total assay time was more than 23 hours as a result of using slow quantification technology (38).

We have shown previously that the antibiotic exposure time in a phenotypic AST can be shortened to 15 min by measuring DNA concentrations in a digital format (26). That work was performed with bacterial UTI isolates and required a 2-hour measurement step using commercial droplet digital polymerase chain reaction (dPCR). The transition from cultures of clinical isolates to clinical samples is invariably challenging for phenotypic AST methods, and previous works have highlighted these challenges (28, 38, 39).

Here, we asked and answered two salient questions: For clinical samples, (i) can digital single-molecule counting of pathogen DNA enable phenotypic AST after a short (15 min)

antibiotic exposure, and (ii) is there a quantification strategy faster than PCR that can be used in a digital format to achieve a pathogen-specific, sample-to-answer phenotypic AST within 30 min directly from a clinical sample? To answer these questions, we developed an ultrafast digital isothermal amplification assay to shorten the readout step and demonstrated that the entire contiguous sample-to-answer workflow could enable an AST result in less than 30 min from a clinical UTI urine sample. We tested the rapid digital loop-mediated isothermal amplification (dLAMP) assay we developed with 51 clinical UTI urine samples and compared the results to commercial dPCR analysis.

RESULTS

Key processes and operational space of digital AST

A phenotypic AST consists of two key processes: antibiotic exposure and measurement of the AST marker. To meet the demands of a rapid AST, these two processes, plus sample handling, must occur within 30 min. The workflow of the digital AST (dAST) method involved the following steps: aliquoting and diluting a clinical urine sample into two equal volumes of media—one with an antibiotic and a control without antibiotic; incubation at 37°C for 15 min; quantification of a target NA sequence (AST marker) in each sample; and calculation of the ratio of the marker concentrations in the control and antibiotic-treated samples, defined as the control/treated (CT) ratio (Fig. 1A).

Antibiotic susceptibility was determined by comparing a CT ratio to a previously determined threshold value (susceptibility threshold). Sample pairs that yield a CT ratio that falls above this threshold are called susceptible, and samples with a ratio below this threshold are called resistant. A CT ratio that is higher than the susceptibility threshold shows that DNA replication continued in the control (−ABX) sample but was slowed or halted in the antibiotic-treated (+ABX) sample, indicating that the sample was susceptible to that antibiotic. CT ratios lower than the susceptibility threshold indicate that DNA replication continued in both the control (−ABX) and antibiotic-treated (+ABX) samples at the same rate, indicating that the sample was resistant to that antibiotic (Fig. 1A, step 4).

The time period of the antibiotic exposure step affects the resolution requirements for the quantification step: A shorter antibiotic exposure results in a smaller difference in the concentration of the target AST marker between the antibiotic-treated and control samples. Thus, at shorter exposure periods, quantification with higher resolution is required to reliably quantify an AST marker. To illustrate the interplay of antibiotic exposure time and required measurement resolution, we explored the trade-off of these three parameters (exposure time, required resolution, and DNA replication rate) computationally and made predictions about the resolution needed to detect susceptibility. We defined this combination of parameters as the operational space (Fig. 1B). For simplicity, we assumed that for an antibiotic-susceptible pathogen, DNA replication halts upon exposure to the antibiotic. Under this assumption, the DNA replication rate (which differs for different pathogens) directly determines the CT ratio at a given antibiotic exposure time. We also assumed that there was no lag phase upon transitioning from urine to liquid media; if there is a lag phase, then the requirements for resolution become even more stringent, further emphasizing the need for high-precision digital measurements. For example, if the measurement method is

limited to twofold resolution, such as in quantitative PCR (qPCR), and the pathogen's DNA doubles every 30 min, then the minimum exposure time necessary to achieve a CT ratio of 2 is 30 min. If the measurement method can instead resolve a 1.2-fold difference in concentrations, then the minimum exposure time decreases to 8 min. Measuring changes in DNA concentration with high resolution therefore allows the detection of a pathogen's response to antibiotic even faster than cell division time (26). Compared with bulk methods (such as qPCR or isothermal amplification), digital quantification can resolve the difference between the two concentrations with greater precision (26, 40, 41), which in turn enables shorter antibiotic exposure times (26).

Digital quantification achieves higher resolution by partitioning target molecules into thousands of compartments such that each compartment contains a single molecule. Amplifying each partitioned molecule to a detectable concentration and counting the number of positive compartments at the end point yield precise quantification. Resolution can be increased, and antibiotic exposure time reduced, by increasing the number of digital compartments. However, the benefit of adding more digital compartments decreases beyond ~1000 compartments, and additional compartments are better used for multiplexing of multiple markers or antibiotics. For example, at UTI-relevant concentrations of DNA (10^6 copies/ml), 1000 digital compartments with 1-nl volume each provides 1.23-fold resolution. Increasing the number of these compartments to 10,000 or 100,000 while correspondingly reducing their volumes to 0.1 and 0.01 nl each, to maintain the same sample volume and total number of target molecules, provides 1.18- and 1.17-fold resolution, respectively (fig. S1). With 10,000 1-nl compartments, the resolution is 1.08, whereas 2000 1-nl compartments provide a resolution of 1.16 each, enabling a fourplex dAST (one control and four antibiotic-treated samples) to be performed with the same number of wells (fig. S1C).

We have previously demonstrated that a 15-min exposure step is sufficient to generate detectable differences in DNA concentrations between the control and antibiotic-treated samples using UTI isolates and four antibiotics commonly prescribed for UTIs (26). For a 15-min exposure period, which is shorter than the fastest reported uropathogenic *Escherichia coli* doubling time of 16 min (42), we predicted the DNA concentration in the control sample to increase 1.4× to 1.6× (Fig. 1B, green star). Other uropathogenic organisms have doubling times of 13 min *(Klebsiella pneumoniae)*, 25 min *(Proteus mirabilis)*, and 29 min *(Staphylococcus saprophyticus)* (43, 44). Therefore, theoretical estimates suggested that a 15-min exposure should provide a 1.4- to 2.2-fold change, which is within the resolution of digital measurements. Historically, such measurements have required 90 min or more (45, 46). For the total assay time to remain less than 30 min, digital NA quantification must be performed in less than 10 min, assuming sample handling (including NA extraction) of at least 5 min and an antibiotic exposure of 15 min. On the basis of these theoretical calculations, we developed a method of digital NA quantification that could be performed in less than 10 min.

dAST in the presence of commensal organisms

A factor that may challenge phenotypic ASTs that are run directly on clinical samples is that commensal or contaminating organisms present in the sample may respond differently to a

given antibiotic than the target pathogen. If the measurement method cannot differentiate between the response of the target pathogen and commensals, then susceptibility cannot be determined accurately. NA amplification can be designed to target a sequence specific to a potential pathogen species or families of interest. Therefore, we hypothesized that when using a pathogen-specific NA target, the CT ratio (and, therefore, the determination of the pathogen as susceptible or resistant by the AST) would not be affected by varying amounts of commensal bacteria. dAST was performed in the presence of *Lactobacillus jensenii* (*Lj*), a common commensal bacterium found in urine. An *E. coli* culture [~10^6 colony-forming units (CFU)/ml] was mixed with each of the three concentrations of *Lj* (0.1×, 1×, and 10x the optical density of the target pathogen) and exposed to cip for 15 min. The response was measured using droplet dPCR, and susceptibility of *E. coli* was determined correctly at all concentrations of the commensal organism (Fig. 2).

Optimization of isothermal amplification (LAMP)

We next focused on shortening the measurement time from 2 hours (time of amplification using dPCR) to <10 min. We investigated dLAMP first because it has been demonstrated previously by us and others (40, 47–50). However, these dLAMP assays previously took >45 min and were not shown to resolve small differences (~1.5×) in NA concentrations. Fast LAMP reactions often show background amplification in negative control experiments, so we aimed to also solve this problem.

We designed primers and optimized real-time LAMP in bulk solutions to maximize amplification speed while eliminating background amplification. At very high NA concentrations, real-time bulk LAMP assays have been reported to be as fast as 5 min (18, 51), but at the lower concentrations of a single target molecule present in a single digital partition (~1 copy/nl = 10^6 copies/ml), amplification takes 10 min or more (52–55). To mimic the concentration of a template in a single digital partition, we performed our bulk optimization experiments at ~10^6 copies/ml. We selected the *E. coli* 23S ribosomal DNA gene as the pathogen-specific NA sequence (dAST marker) and as the target for primer design because we showed previously that this was a reliable marker for DNA replication in the context of AST (26). Pan-Enterobacteriaceae primers would be useful for targeting other UTI pathogens. Although we did not purposefully design our primers to exclude other Enterobacteriaceae pathogens, we were able to detect *K. pneumoniae* and P. *mirabilis* in pilot experiments using the same primers. Sensitivity and specificity of these primers remain to be further validated for additional pathogens and commensals.

The LAMP optimization process (Fig. 3A) consisted of four steps: (1) screening multiple LAMP primer sets for speed and lack of background amplification, (2) screening multiple loop primer pairs with the selected primer set from step 1 for speed and lack of background amplification, (3) testing the selected LAMP and loop primers with a range of magnesium ion (Mg) concentrations, and (4) selecting the optimal amplification temperature from the data obtained in step 3. Each parameter was tested using a temperature gradient, which proved to be critical to minimizing the time to positive (TTP), the reaction time to detect a positive sample. Of the four tested LAMP primer sets, we selected set B because it showed the fastest amplification and no background amplification (Fig. 3A, step 1). No loop primer

pair showed much earlier TTPs than any other pair, and no pair showed theoretical or experimental evidence of primer-dimers, so we arbitrarily chose the loop A set (Fig. 3A, step 2). Four concentrations of Mg were tested using the DNA polymerase Bst 3.0. The resulting TTPs varied by as much as 11 min depending on the amplification temperature. This optimization process resulted in TTPs as fast as ~4 to 5 min for ~700 target copies in a 6-μl amplification volume, with the fastest TTP (4.4 min) obtained using 6 mM Mg at 71°C.

Once LAMP primers and protocols had been optimized, we further tested their specificity for the dAST marker. No positive signals were obtained when we ran real-time LAMP using L*j* genomic DNA (gDNA), human gDNA, or urine from healthy donors without any symptoms of UTI (Fig. 3B). When testing clinical UTI samples, a positive signal was only obtained when *E. coli* DNA was present. TTPs ranged from 4 to 5 min for clinical UTI samples (Fig. 3C). However, using this LAMP method in a standard well-plate format to resolve a 1.5× difference in concentration would require detecting a difference in TTP of ~8 s, which is difficult in practice to perform robustly (40).

dAST using ultrafast single-molecule counting (dLAMP)

Our next goal was to test whether using this optimized LAMP chemistry in a digital format would yield an accurate determination of antibiotic susceptibility while preserving the speed observed in bulk solutions. This would require the ability to resolve small changes in NA concentrations that occur after a 15-min exposure to antibiotic, despite any heterogeneity in TTPs (the difference in amplification kinetics of individual molecules), which has been observed previously (50, 56). Because sample matrices might increase the heterogeneity in TTPs and thus decrease the resolution, we tested clinical urine samples, which can contain urea, proteins, blood (including heme as a potent PCR inhibitor), and other cellular components that can interfere with assay detection. To eliminate extracellular DNA present in clinical urine as a potential source of error, we modified the dAST procedure that we previously developed for isolates (26) to include deoxyribonuclease (DNase) during the exposure step to digest any extracellular DNA (see the Supplementary Materials). We used the optimized LAMP assay (Fig. 3) with SlipChip microfluidic devices in a digital format (57). The SlipChip partitioned the samples into 1280 digital compartments. In each compartment, single molecules were amplified ifpresent, and the total number of positive compartments was counted in real time (56). In a clinical setting, decisions are typically made from single assay runs, and thus, we tested whether differences in NA concentrations between the control and antibiotic-treated samples could be resolved reliably using a single 1280-well SlipChip for each measurement.

Using dLAMP (Fig. 4), most (>80%) single molecules amplified between 4 and 10 min, as shown by the fluorescence curves plotted in Fig. 4 (A and F). As expected, heterogeneity in TTP was observed, likely as a result of the stochasticity of single-molecule amplification (50, 58). Despite heterogeneity and matrix effects of clinical urine, we detected a significant difference in NA concentration ($P = 6.1 \times 10^{-4}$) after only 5 min of amplification time for the cip-susceptible clinical urine sample (Fig. 4C). For the cip-resistant sample, no significant difference in concentration was detected during the dLAMP assay ($P > 0.05$) (Fig. 4H). In both samples, the CT ratios were stable after 6 min and 40 s (6.7 min) of amplification (Fig.

4, D and I), were consistent with the ratios obtained by dPCR (Fig. 4, E and J), and yielded the correct AST call (susceptible or resistant). We then repeated this dLAMP assay for one nit-susceptible and one nit-resistant clinical urine sample. After 6.7 min of dLAMP amplification time, the CT ratios for both samples were stable, and the correct antibiotic-susceptibility call was determined (fig. S2). This demonstrates that the optimized dLAMP assay yields correct AST calls in only 6.7 min, below the 10-min limit necessary to achieve a 30-min dAST. Further, individual DNA target molecules were detected, and the DNA concentration was accurately quantified even after dilution during antibiotic exposure and sample preparation (table S1).

Thirty-minute sample-to-answer dAST directly from clinical urine samples

Next, we tested whether the entire dAST workflow (antibiotic exposure, sample preparation, measurement, and data analysis) could be performed in less than 30 min (Fig. 5). To accomplish this goal, we shortened the sample preparation time from 10 to 2 min while maintaining compatibility with dLAMP. In parallel with antibiotic exposure of a clinical sample, rapid real-time LAMP was used to confirm the presence of *E. coli* and to measure the approximate NA concentration of the dAST marker in the sample (Fig. 5B). This step provided the identification of the pathogen and could be used to select the amount of NAs loaded on the chip to maximize the performance of the digital assay without adding time to the workflow; it also avoided the AST quantification step for the samples lacking the pathogen or containing subclinical amounts. We also modified the real-time image analysis software we developed previously (56) to calculate the concentrations of the dAST marker in real time from each image, instead of after completion of amplification.

After these modifications, we calculated that all steps could be performed within ~24 min [15 min (exposure) + 2 min (sample preparation) + 6.7 min (readout)]. We tested whether these steps could be performed in succession to provide a full sample-to-answer workflow, including all fluid transfer steps and data analysis, within 30 min. We started a timer when an infected clinical urine sample was added to media with and without cip. After 29.8 min of total elapsed time (6.7 min of dLAMP amplification time), the software reported the control and treated concentrations for the cip-susceptible sample to be significantly different ($P = 7.4\times 10^{-10}$), with a CT ratio of 1.59. For the cip-resistant sample, no significant difference in concentration was reported through the entire dLAMP assay ($P > 0.05$). At 29.2 min (6.7 min of dLAMP amplification time), the CT ratio for the cip-resistant sample was 1.08 (Fig. 5D). This result shows how a combination of rapid partitioning, fast isothermal amplification, and high-resolution digital measurements enabled antibiotic susceptibility to be determined in less than 30 min.

dAST using a set of 51 clinical samples

Having established that the dAST method could be performed, sample-to-answer, in less than 30 min, we next tested dAST with 51 clinical samples using both dPCR and dLAMP readouts. Samples were exposed to antibiotic for 15 min, and NA extraction was performed on a total of 51 clinical UTI samples containing $\geq 5 \times 10^4$ CFU/ml *E. coli* (17 cip-susceptible, 14 cip-resistant, 18 nit-susceptible, and 5 nit-resistant). Three clinical samples were tested separately with cip and nit, for a total of 54 tests. We focused on categorical

agreement of our binary susceptibility determination (susceptible or resistant) and did not test intermediate samples due to the variability in minimum inhibitory concentration (MIC) determination of gold standard AST methods (59, 60). It is common to only challenge new AST methods against susceptible and resistant samples (34,35, 61), which excludes a small fraction of samples for cip (62). To ensure that there were no special issues with bacteria with intermediate MICs, we used the dAST method on a small set of cip-intermediate isolates to better understand its performance (fig. S3).

We quantified the DNA AST marker of the control and treated extractions on all 54 samples with both dPCR and dLAMP. For each sample, the CT ratio was calculated and compared to a susceptibility threshold [1.10; determined in (26)] to classify the samples as resistant or susceptible (Fig. 6A). Discordant CT ratios were observed for five samples when compared with the gold standard broth microdilution method. To resolve the discrepancy, we reran three of these five discordant samples, averaging the second CT ratio with the CT ratio from the first run to obtain a consensus value of the CT ratio (table S2, samples #28, #29, and #36). As a control, we also reran one sample that was not discordant (table S2, sample #122). To ensure clinical samples yielded reproducible CT ratios, we used the dAST method to test a small set of cip-susceptible isolates in triplicate (fig. S4).

With 1.10 as the susceptibility threshold for dPCR measurements, the dAST method returned 51 correct calls (94.4% categorical agreement), 2 very major errors for 19 resistant samples (10.5%), and 1 major error for 35 susceptible samples (2.9%). Because 1.10 was a threshold based on experiments with isolates (26), we generated a receiver operating characteristic (ROC) curve to inform the optimal threshold for clinical UTI samples (Fig. 6B). ROC curves show the ability of a diagnostic test to discriminate positives and negatives based on a threshold: Values below the threshold are called negative (resistant), and values above the threshold are called positive (susceptible). The area under the curve (AUC) for the generated ROC was 0.98. Using the optimal threshold given by the ROC curve (1.14), 53 of 54 dAST calls matched the gold standard AST call (98.1% categorical agreement) with 1 very major error (5.3%) and 0 major errors (0%).

We also used dLAMP to quantify the same 54 samples. The CT ratios at 6.7 min were calculated and plotted in Fig. 6C, along with the ROC curve for dLAMP (Fig. 6D). With 1.10 as the susceptibility threshold for dLAMP measurements at 6.7 min, the dAST method returned 51 correct calls (94.4% categorical agreement), 2 very major errors for 19 resistant samples (10.5%), and 1 major error for 35 susceptible samples (2.6%). The AUC for the generated ROC curve was 0.96. Using the optimal threshold given by the ROC curve (1.11), 52 of 54 dAST calls matched the gold standard AST call (96.3% categorical agreement) with 1 very major error (5.3%) and 1 major error (2.9%). These data show that although the optimal thresholds derived from the ROC curves (1.14 for dPCR and 1.11 for dLAMP) slightly improve the categorical agreement, they are consistent with the threshold established for isolates [1.10 (26)] and are consistent with each other. Quantifying DNA with dLAMP at 6.7 min produces similar CT ratios and susceptibility calls as dPCR.

DISCUSSION

Here, we solved three problems to determine phenotypic antibiotic susceptibility in clinical samples within 30 min. First, we used digital quantification of a DNA marker to reduce the antibiotic exposure time to 15 min. Second, we showed that dAST is robust to the presence of commensal bacteria and clinical urine matrices. Third, we developed and optimized a rapid, high-resolution measurement method for quantifying NA targets that shortens the measurement step to less than 10 min.

The dLAMP assay developed here was capable of amplifying single target DNA molecules in less than 5 min. Despite the heterogeneity of single-molecule amplification times, high-resolution measurements were obtained even before all partitions with a target DNA molecule had amplified (~6.7 min). This makes dLAMP a strong tool for real-time, high-resolution, rapid measurements of NAs. Rapid, high-resolution measurements increase the information gained in shorter times and will be invaluable for other assays, such as viral load measurements and genotyping (50, 63, 64). LAMP was chosen for translation to a digital format because it is a well-established amplification chemistry (51, 65, 66) with several readout methods (67–70). If necessary, other amplification chemistries—including NASBA (NA sequence-based amplification), RPA (recombinase polymerase amplification), NEAR (nicking enzyme amplification reaction), and HDA (helicase-dependent amplification)—could be tested and optimized for a digital format and used to measure a marker of interest. Additionally, we show that the LAMP assay is compatible with a rapid, one-step extraction method, which considerably reduces the sample preparation time. Because of the speed of extraction and amplification, the same LAMP assay can be used in a real-time bulk format for rapid pathogen identification in parallel with the 15-min antibiotic exposure step. This step, completed in <10 min including sample preparation, did not extend the total assay time but provided two critical pieces of information before digital quantification: (i) whether a sample was infected with the pathogen of interest and (ii) whether a sample contained clinically relevant concentrations of the pathogen. UTI-positive samples gave TTP values of 4 to 5 min (corresponding to ~10 to 10 DNA copies/ml, n = 7) (Fig. 3C), whereas healthy urine samples remained negative for at least 20 min (n = 5) (Fig. 3B). This specificity is critical in working with clinical samples because it enables the dAST to provide information specific to the pathogens of interest rather than commensals, contaminating organisms, or mixtures of pathogens. Additionally, using dLAMP to calculate the CT ratios and determine susceptibility was informative for estimating pathogen concentration in the urine sample (see table S1).

Most of the previous rapid AST methods used cultures of clinical isolates instead of clinical samples (see table S3 for a quantitative summary of the published state of the art). The introduction of commensal or contaminating organisms and clinical sample matrices to diagnostic workflows can cause major challenges in the development and translation of laboratory methods. It is therefore critical to prove that AST methods are compatible with clinical samples. Here, we have shown that the dAST method is compatible with a wide range of urine samples. Urine color of the samples included colorless, yellow, dark yellow, and red; pH ranged from <5.0 to 8.0; and protein concentrations ranged from 0.0 to 1.0 mg/ml (71). Additionally, red and white blood cell counts were as high as $>10^6$ cells/ml each

in separate samples, and several samples demonstrated elevated glucose. One sample contained a lactose-positive Gram-negative rod bacterium (3×10^4 CFU/ml) in addition to the infecting *E. coli*. Although this study warrants more extensive follow-up investigation into more detailed correlations between urine composition and dAST speed and does not establish whether this method would work in a more complex matrix like whole blood, our results indicate that dAST is compatible with a wide range of urine matrices and contaminants in clinical samples.

The dAST method described herein was demonstrated with a specific scenario, and thus, there are inherent limitations to the extrapolations we can make to other pathogens and antibiotics. These limitations will guide future work in this area. We demonstrated dAST using a single clinical sample set of UTI urine samples infected with *E. coli*, which causes 80% of UTIs, using a threshold of 1.10 previously established with isolates. This is similar to other studies at this stage of technology development (72–74); multiple clinical sets should be run in the future.

Cip was chosen because it has become one of the most commonly prescribed antibiotics for UTIs, despite being a second-line therapy that should be preserved for more severe cases (12, 13, 75). Nit was chosen because it is the recommended treatment for acute uncomplicated cystitis (6). Nit is a highly effective first-line antibiotic that is often overlooked because of a lack of susceptibility data. The lack of AST data becomes especially important because nit is sometimes used as a prophylactic treatment for recurrent UTIs and, despite its effectiveness, is not used to treat acute cases due to susceptibility concerns (12). Multiplexing with more pathogens and antibiotics in a blinded study is an important next step that, if successful, would further validate and prove the clinical utility of this rapid dAST assay.

Other UTI pathogens may have slower growth rates and smaller differences in control and treated concentrations (Fig. 1B); however, these differences are theoretically resolvable with digital NA quantification. Furthermore, alternative dAST markers might yield larger CT ratios after shorter antibiotic exposure times. In particular, changes in RNA in response to antibiotic exposure have been shown to be both large and fast (38) and should be rapidly discernable with digital methods such as the ones described here. For example, we have demonstrated quantification of viral RNA on digital SlipChips (64, 76), including a 5-plex chip for multiplexed measurements. With chip designs properly adjusted for appropriate multiplexing and desired resolution (fig. S1), multiplexed measurements could be useful for analyzing combinations of RNA markers (38). Additionally, RNA markers (38) and alternative DNA markers may be required for antibiotics with different mechanisms of action, such as β-lactams (26), to achieve a 30-min sample-to-answer dAST.

Pathogen concentration is also considered when working with clinical samples. Quantifying NAs with high resolution is challenging if the NA concentration drops below the optimal dynamic range of the system. For example, in sepsis, the concentration of pathogens in blood can be as low as ~1 to 10 CFU/ml (77). Although blood cultures, which require overnight or longer incubations, are currently used to increase the concentration of pathogens, they are too slow to inform the initial treatment because each additional hour of

delayed treatment in sepsis results in a 7.6% increase in mortality (25), emphasizing the need for rapid AST. This major challenge of low concentrations of pathogens must be overcome to perform dAST in cases of sepsis and will require alterations to the methodology, such as the addition of a pathogen-concentrating step before antibiotic exposure. Last, we have not tested dAST against heteroresistant microbial populations, which have been documented in Gram-positive organisms (78) but are not common in Gram-negative organisms.

We have streamlined many aspects of the workflow for the dAST demonstration and believe this workflow can be performed by trained personnel in diagnostic laboratories. However, because this process requires several pipetting and handling steps, operator error is possible. We anticipate that dAST would have the greatest impact on antibiotic stewardship if it could be performed by minimally trained personnel at the POC. This would require integration of the dAST workflow into an inexpensive, simple-to-use device operated with inexpensive equipment. An integrated dAST device would increase throughput and reduce the potential biohazard risks associated with open pipetting steps, which are a limitation of our current protocol. Although not demonstrated here, an integrated device should be feasible due to the straightforward nature of the dAST workflow. Isothermal digital quantification can be performed using a range of technologies and amplification chemistries (40, 47, 49, 63, 79), including SlipChips, which are compatible with untrained users (80) and can be read with inexpensive optics such as a camera phone (40, 70). Whereas reusable glass SlipChips require cleaning (76), disposable injection-molded SlipChips further simplify the workflow. Furthermore, the SlipChip platform supports multiplexed digital measurements (45), which is desired to perform AST on multiple antibiotics and/or pathogens simultaneously. Finally, the robustness of isothermal digital amplification to temperature, imaging conditions, reaction time (40), sample preparation methods (81, 82), and inhibitors (83–85) could further simplify the instrument requirements. This rapid dAST, if fully developed and validated for additional microorganisms, antibiotics, and sample types and transitioned to a Clinical Laboratory Improvement Amendments-waived POC device approved by the regulatory bodies, would enable rapid clinical decision-making, improve management of infectious diseases, and increase antimicrobial stewardship.

MATERIALS AND METHODS

Study design

The objective of this study was to develop a rapid phenotypic AST using digital NA quantification. The two key hypotheses of this work were as follows: (i) 15 min of antibiotic exposure can cause sufficient differences in pathogen-specific DNA concentrations between control and antibiotic-treated samples such that a high-resolution digital quantification measurement method such as dPCR can reliably detect a difference in NA concentrations for a susceptible sample and (ii) a rapid dLAMP assay can resolve these small differences in NA concentration in less than 10 min. To test the first hypothesis, 51 clinical human urine samples were tested using the dAST method (three samples run with both antibiotics for a total of 54 antibiotic-susceptibility calls), and the results were compared to the gold standard broth micro-dilution. Clinical UTI samples with *E. coli* as the pathogen of interest were

chosen as a test case for the dAST method using one first-line antibiotic (nit) and one second-line antibiotic (cip). To test the second hypothesis, the rapid dLAMP assay was compared with a commercial dPCR system for calculating the CT ratios and determining antibiotic susceptibility from clinical UTI samples.

To calculate the sample size, the methods and Equation 5 from (86) were used. We define the true-positive rate (sensitivity) as the proportion of gold standard-susceptible samples that are correctly identified as susceptible by the dAST method and the true-negative rate (specificity) as the proportion of gold standard-resistant samples that are correctly identified as resistant by the dAST method. We suspected that the specificity and sensitivity of the dAST method would be 95% with a desired margin of error of ±10%. Under these conditions, 18.2 (or 19) samples must be tested with the dAST method and compared to the gold standard. We tested 19 resistant samples and 35 susceptible samples. Experimental details of LAMP primer design, optimization, and specificity and the rapid dLAMP assay are described in the Supplementary Materials.

dAST in the presence of commensal organisms

Antibiotic-susceptible and antibiotic-resistant isolates of *E. coli* from patients diagnosed with UTIs were obtained from the University of California, Los Angeles, Clinical Microbiology Laboratory (UCLA CML). These isolates were treated separately with and without antibiotics (±ABXs) in the presence of varying concentrations of Lj (also isolated from a clinical UTI urine sample by the UCLA CML). *Lj* was spiked into clinical urine samples at varying concentrations relative to the concentration of *E. coli*. Concentrations were determined by measuring the optical density at 600 nm. Samples were exposed to cip (1 mg/ml; Sigma-Aldrich) for 30 min (26). A 10-ml aliquot of the sample was removed after 0, 15, and 30 min of exposure and added to 90 μl of QuickExtract DNA Extraction Solution (Epicentre). Target DNA was quantified using droplet dPCR (26). The fold change in the concentration of target DNA after 15 min of antibiotic exposure relative to time 0 in the control and antibiotic-treated samples was compared (Fig. 2, A and B), measuring the significance of this difference by *P* value as described previously (26). The CT ratios at 15 min (Fig. 2C) were calculated as the ratios of the marker concentrations in the control and antibiotic-treated samples.

The primers used for all dPCR amplification experiments target the 23S gene of the Enterobacteriaceae family (26). The concentrations of the components in the dPCR mix used for these experiments and all subsequent dPCR experiments were as follows: 1× QX200 ddPCR EvaGreen Supermix (Bio-Rad), 500 nM forward primer, and 500 nM reverse primer. The NA extraction comprised 10% of the final volume in the dPCR mix. The remaining volume was nuclease-free water (NF-H_2O).

dAST using clinical UTI samples

Clinical urine samples were obtained under an approved institutional review board (IRB) protocol at the UCLA CML (#15–001189) and analyzed at the California Institute of Technology (Caltech) under an approved protocol (IRB #15–0566). Samples were deidentified before being transported to Caltech. Samples were stored in Vacutainer Plus

C&S Boric Acid Sodium Borate/Formate tubes (Becton Dickinson), transported at ambient temperature, and stored at 4°C once received at Caltech. Urine samples were from otherwise healthy patients suspected of having a UTI (based on urinalysis results). The presence of *E. coli* was confirmed by the UCLA CML, and MICs were determined as described previously (26). Urine samples were selected for dAST analysis based on the determined MIC of the infecting *E. coli*. Samples were considered cip-susceptible if the determined MIC was ≤0.25 μg/ml and considered cip-resistant if the MIC was ≥ 4 μg/ml. Samples were considered nit-susceptible if the MIC was ≤ 16 μg/ml and considered nit-resistant if the MIC was ≥ 128 μg/ml. Viable bacteria are a requirement of phenotypic ASTs. Nonviable samples were excluded if a decrease in DNA concentration was observed (indicating digestion of DNA from nonviable cells). If the change in DNA concentration was not easily discernible by dPCR after 15 min of growth in media, then the DNA concentration at 30 min was measured to determine whether the sample was viable (DNA concentration increased at 30 min) or nonviable (DNA concentration decreased at 30 min).

Before the start of each experiment, urine as received, still containing boric acid, was warmed to 37°C over 30 min to mimic the temperature of fresh urine samples. At the start of each dAST experiment ($t = 0$), warmed urine was added to media (prewarmed to 37°C) with or without antibiotics (±ABXs) to initiate DNA replication and begin exposure. This addition to media dilutes the boric acid in the transport media, allowing bacterial replication to proceed. The final 500-μl sample mixture in the control and treated tubes contained 250 μl of brain heart infusion media (Becton Dickinson), 25 μl of DNase I (New England Biolabs), 5 μl of DNase buffer (100 mM tris-HCl, 25 mM $MgCl_2$, and 5 mM $CaCl_2$), and an aliquot of the urine, with the remaining volume of NF-H_2O. Either cip (1 mg/ml) or nit (16 mg/ml) was added to the +ABX sample, with an equal volume of NF-H_2O (in the case of cip) or dimethylformamide (in the case of nit) added to the control sample (−ABX). Antibiotic concentrations were chosen on the basis of our previous work with isolates (26) and are near the Clinical and Laboratory Standards Institute and European Committee on Antimicrobial Susceptibility Testing breakpoints. A 10-ml aliquot of urine was added to control and treated tubes in the cip treatments, and a 25-μl aliquot was added in the nit treatments. Samples were shaken at 750 rpm at 37°C for 30 min. After 0, 15, and 30 min of exposure, 10-μl aliquots of the control and treated samples were removed and added to 90 μl of QuickExtract DNA Extraction Solution. The extracted samples were heated according to a modified version of the manufacturer's protocol (65°C for 6 min, 95°C for 4 min, and chilled on ice), vortexed, and centrifuged. Next, 5 μl of each extraction was added to 45 ml of ddPCR mix and quantified using dPCR. If the DNA concentration of the sample was too high, then the template was diluted in NF-H_2O and dPCR was rerun. The CT ratios were calculated; if the dAST call did not match the gold standard AST call, then the sample was rerun several hours later on the same day. For the four samples that were rerun, only the second set of NA extractions were quantified by dLAMP.

Sample-to-answer dAST in less than 30 min

Clinical urine samples were treated with ("treated") and without ("control") cip (1 μg/ml) for 15 min as described above. A timer was started as soon as urine was added to the media with and without cip. After 0 and 15 min, a 20-μl aliquot of each sample was added to 80 μl of

QuickExtract DNA Extraction Solution (Epicentre). The two samples were then heated at 65°C for 1 min followed by 98°C for 1 min, after which they were chilled by incubation on an ice block for 30 s, vortexed, and centrifuged.

In parallel with the 15-min antibiotic exposure step, we used the semiquantitative ability of quantitative LAMP to predict the appropriate dilution factor for our 1280-well digital SlipChips. A 2-μl aliquot from each of the control and treated DNA extractions from time 0 was added to 8 ml of LAMP mix. The samples, along with two standards with known DNA concentrations (S1, 128.5 copies/ml; S2, 766.0 copies/ml), were then incubated at 72°C for 5 min on a Roche LightCycler 96, and fluorescent traces were monitored in real time. If the TTP of the average of the samples was earlier than the TTP of S1, then 3 ml of the NA aliquot extracted at 15 min was added to 24 μl of dLAMP mix, along with 3 ml of NF-H_2O. If the TTP of the sample was between the TTPs of S1 and S2, then 6 ml of the 15-min NA extraction was added to 24 μl of dLAMP mix, with no additional NF-H_2O added. This step was completed within the 15 min of antibiotic exposure. In the experiments with both antibiotic-resistant and antibiotic-susceptible samples (Fig. 5), the TTP was earlier than the TTP of S1.

After semiquantification and mixture of the dLAMP mix with the template, the dLAMP solutions were pipette-mixed, loaded into SlipChips, partitioned into 1280 compartments, and placed on the thermal cycler of a digital real-time imaging instrument at 72°C.

Images were taken every 26 s, and concentrations were calculated on the basis of the number of positive and negative wells [as described in Rapid digital LAMP (dLAMP) in the Supplementary Materials]. Software developed in (56) was modified to enable real-time image processing and concentration calculations as each image was taken instead of after the assay completed. The CT ratios were also calculated for each time point; the value of the CT ratio after 6.7 min of amplification time is plotted in Fig. 5D and was compared to a threshold of 1.10 to determine susceptibility or resistance. The timer was stopped at this time point; 29.8 min had elapsed when running dAST with the susceptible sample, and 29.2 min had elapsed with the resistant sample.

Statistical analysis

Poisson statistics was used to calculate the 95 or 98% confidence interval of the NA concentration for each digital measurement (45). To calculate the error in fold change, we used standard error propagation methods (87). With λ as a concentration and σ as the SD, the equation is

$$\sigma_{\text{ratio}} = \sqrt{\left(\frac{\sigma_{\lambda_2}}{\lambda_1}\right)^2 + \left(\frac{\lambda_2 \cdot \sigma_{\lambda_2}}{\lambda_1^2}\right)^2}$$

Kreutz *et al.* (45) demonstrated that results from a Z test (assuming a normal distribution) and a permutation test are in very good agreement for various SlipChip designs; therefore, it is appropriate to calculate P values comparing digital NA concentrations with a one-sided Z

test. This Z test asks whether the control NA concentration ($\lambda_{control}$) is 1.10× higher than the treated NA concentration (λ_{ABX}) (26, 45)

$$Z = \frac{\ln(\lambda_{control}) - \ln(1.10 \cdot \lambda_{ABX})}{\sqrt{\sigma^2_{\ln(\lambda_{control})} + \sigma^2_{\ln(\lambda_{ABX})}}}$$

Concentration (λ) and SD (a) for each digital NA measurement were calculated from the number of positive and negative compartments with Poisson statistics as described in (45) for single-volume digital NA quantification. A significance level of 0.05 was used.

Supplementary Material

Refer to Web version on PubMed Central for supplementary material.

Acknowledgments:

We thank N. Shelby for contributions to manuscript writing and editing, M. Lee at the Clinical Microbiology Laboratory at UCLA for assistance with clinical sample and data acquisition, SlipChip Corp. for providing injection-molded SlipChips for dLAMP quantification, and W. Liu and D. Capule of SlipChip Corp. for providing technical assistance and expertise.

Funding:

This research was supported by the Defense Advanced Research Projects Agency (DARPA) Cooperative Agreement HR0011-11-2-0006, NIH grant R01EB012946, a Burroughs Wellcome Fund Innovation in Regulatory Science award, an NIH National Research Service Award (NRSA) (5T32GM07616NSF) to N.G.S., and a grant from the Joseph J.Jacobs Institute for Molecular Engineering for Medicine.

REFERENCES AND NOTES

1. Laxminarayan R, Duse A, Wattal C, Zaidi AKM, Wertheim HFL, Sumpradit N, Vlieghe E, Hara GL, Gould IM, Goossens H, Greko C, So AD, Bigdeli M, Tomson G, Woodhouse W, Ombaka E, Peralta AQ, Qamar FN, Mir F, Kariuki S, Bhutta ZA, Coates A, Bergstrom R, Wright GD, Brown ED, Cars O, Antibiotic resistance—The need for global solutions. Lancet Infect. Dis 13, 1057–1098 (2013). [PubMed: 24252483]
2. O'Neill J, Tackling drug-resistant infections globally: Final report and recommendations (2016); https://amr-review.org/Publications.html.
3. O'Neill J, Rapid diagnostics: Stopping unnecessary use of antibiotics (2015); https://amr-review.org/Publications.html.
4. Cosgrove SE, The relationship between antimicrobial resistance and patient outcomes: Mortality, length of hospital stay, and health care costs. Clin. Infect. Dis 42 (suppl. 2), S82–S89 (2006). [PubMed: 16355321]
5. Perez KK, Olsen RJ, Musick WL, Cernoch PL, Davis JR, Land GA, Peterson LE, Musser JM, Integrating rapid pathogen identification and antimicrobial stewardship significantly decreases hospital costs. Arch. Pathol. Lab. Med 137, 1247–1254 (2013). [PubMed: 23216247]
6. Gupta K, Hooton TM, Naber KG, Wullt B, Colgan R, Miller LG, Moran GJ, Nicolle LE, Raz R, Schaeffer AJ, Soper DE; Infectious Diseases Society of America; European Society for Microbiology and Infectious Diseases, International clinical practice guidelines for the treatment of acute uncomplicated cystitis and pyelonephritis in women: A 2010 update by the Infectious Diseases Society of America and the European Society for Microbiology and Infectious Diseases. Clin. Infect. Dis 52, e103–e120 (2011). [PubMed: 21292654]

7. Centers for Disease Control and Prevention (CDC), Antibiotic resistance threats in the United States (CDC Office of Infectious Diseases, 2013); www.cdc.gov/drugresistance/pdf/ar-threats-2013-508.pdf.
8. Nesta, Longitude Prize: How can we prevent the rise of resistance to antibiotics? (2014); https://longitudeprize.org/challenge/antibiotics.
9. Center for Disease Dynamics, Economics and Policy (CDDEP), State of the world's antibiotics (CDDEP, 2015); www.cddep.org/wp-content/uploads/2017/06/swa_edits_9.16.pdf
10. The White House, National action plan for combating antibiotic-resistant bacteria (The White House, 2015); https://obamawhitehouse.archives.gov/sites/default/files/docs/national_action_plan_for_combating_antibotic-resistant_bacteria.pdf
11. World Health Organization (WHO), Global antimicrobial resistance surveillance system— Manual for early implementation (WHO, 2015); http://apps.who.int/iris/bitstream/10665/188783/1/9789241549400_eng.pdf.
12. Barber AE, Norton JP, Spivak AM, Mulvey MA, Urinary tract infections: Current and emerging management strategies. Clin. Infect. Dis 57, 719–724 (2013). [PubMed: 23645845]
13. Hooton TM, Uncomplicated urinary tract infection. N. Engl. J. Med 366, 1028–1037 (2012). [PubMed: 22417256]
14. Kobayashi M, Shapiro DJ, Hersh AL, Sanchez GV, Hicks LA, Outpatient antibiotic prescribing practices for uncomplicated urinary tract infection in women in the United States, 2002–2011. Open Forum Infect. Dis 3, ofw159 (2016). [PubMed: 27704014]
15. Reller LB, Weinstein M, Jorgensen JH, Ferraro MJ, Antimicrobial susceptibility testing: A review of general principles and contemporary practices. Clin. Infect. Dis 49, 1749–1755 (2009). [PubMed: 19857164]
16. Kostic T, Ellis M, Williams MR, Stedtfeld TM, Kaneene JB, Stedtfeld RD, Hashsham SA, Thirty-minute screening of antibiotic resistance genes in bacterial isolates with minimal sample preparation in static self-dispensing 64 and 384 assay cards. Appl. Microbiol. Biotechnol 99, 7711–7722 (2015). [PubMed: 26227406]
17. Ikeuchi T, Seki M, Akeda Y, Yamamoto N, Hamaguchi S, Hirose T, Yamanaka K, Saito M, Tomono K, Tamiya E, PCR-based method for rapid and minimized electrochemical detection of mecA gene of methicillin-resistant Staphylococcus aureus and methicillin-resistant Staphylococcus epidermidis. Gen. Med. (Los Angel.) 3, 215 (2015).
18. Zboromyrska Y, Vergara A, Cosgaya C, Verger G, Mosqueda N, Almela M, Pitart C, Roca I, Marco F, Vila J, Rapid detection of b-lactamases directly from positive blood cultures using a loop-mediated isothermal amplification (LAMP)-based assay. Int. J. Antimicrob. Agents 46, 355–356 (2015). [PubMed: 26141229]
19. Peterson LR, Schora DM, Methicillin-resistant Staphylococcus aureus control in the 21st century: Laboratory involvement affecting disease impact and economic benefit from large population studies. J. Clin. Microbiol 54, 2647–2654 (2016). [PubMed: 27307459]
20. van der Zee A, Hendriks WDH, Roorda L, Ossewaarde JM, Buitenwerf J, Review of a major epidemic of methicillin-resistant Staphylococcus aureus: The costs of screening and consequences of outbreak management. Am. J. Infect. Control 41, 204–209 (2013). [PubMed: 22921104]
21. Spencer M, Barnes S, Parada J, Brown S, Perri L, Uettwiller-Geiger D, Johnson HB, Graham D, A primer on on-demand polymerase chain reaction technology. Am. J. Infect. Control 43, 1102–1108 (2015). [PubMed: 26198577]
22. Davies J, Davies D, Origins and evolution of antibiotic resistance. Microbiol. Mol. Biol. Rev 74, 417–433 (2010). [PubMed: 20805405]
23. Marston HD, Dixon DM, Knisely JM, Palmore TN, Fauci AS, Antimicrobial resistance. JAMA 316, 1193–1204 (2016). [PubMed: 27654605]
24. Hicks JM, Haeckel R, Price CP, Lewandrowski K, Wu AHB, Recommendations and opinions for the use of point-of-care testing for hospitals and primary care: Summary of a 1999 symposium. Clin. Chim. Acta 303, 1–17 (2001). [PubMed: 11163017]
25. Kumar A, Roberts D, Wood KE, Light B, Parrillo JE, Sharma S, Suppes R, Feinstein D, Zanotti S, Taiberg L, Gurka D, Kumar A, Cheang M, Duration of hypotension before initiation of effective

antimicrobial therapy is the critical determinant of survival in human septic shock. Crit. Care Med 34, 1589–1596 (2006). [PubMed: 16625125]

26. Schoepp NG, Khorosheva EM, Schlappi TS, Curtis MS, Humphries RM, Hindler JA, Ismagilov RF, Digital quantification of DNA replication and chromosome segregation enables determination of antimicrobial susceptibility alter only 15 minutes of antibiotic exposure. Angew. Chem. Int. Ed. Engl 55, 9557–9561 (2016). [PubMed: 27357747]
27. Baltekin O, Boucharin A, Tano E, Andersson DI, Elf J, Antibiotic susceptibility testing in less than 30 min using direct single-cell imaging. Proc. Natl. Acad. Sci. U.S.A 114, 9170–9175 (2017). [PubMed: 28790187]
28. Fredborg M, Andersen KR, Jorgensen E, Droce A, Olesen T, Jensen BB, Rosenvinge FS, Sondergaard TE, Real-time optical antimicrobial susceptibility testing. J. Clin. Microbiol 51, 2047–2053 (2013). [PubMed: 23596243]
29. Choi J, Yoo J, Lee M, Kim E-G, Lee JS, Lee S, Joo S, Song SH, Kim E-C, Lee JC, Kim HC, Jung Y-G, Kwon S, A rapid antimicrobial susceptibility test based on single-cell morphological analysis. Sci. Transl. Med 6, 267ra174 (2014).
30. Douglas IS, Price CS, Overdier KH, Wolken RF, Metzger SW, Hance KR, Howson DC, Rapid automated microscopy for microbiological surveillance of ventilator-associated pneumonia. Am. J. Respir. Crit. Care Med 191, 566–573 (2015). [PubMed: 25585163]
31. Chantell C, Multiplexed automated digital microscopy for rapid identification and antimicrobial susceptibility testing of bacteria and yeast directly from clinical samples. Clin. Microbiol. Newsl 37, 161–167 (2015).
32. Ertl P, Robello E, Battaglini F, Mikkelsen SR, Rapid antibiotic susceptibility testing via electrochemical measurement of ferricyanide reduction by Escherichia coli and Clostridium sporogenes. Anal. Chem 72, 4957–4964 (2000). [PubMed: 11055715]
33. Halford C, Gonzalez R, Campuzano S, Hu B, Babbitt JT, Liu J, Wang J, Churchill BM, Haake DA, Rapid antimicrobial susceptibility testing by sensitive detection of precursor rRNA using a novel electrochemical biosensing platform. Antimicrob. Agents Chemother 57, 936–943 (2013). [PubMed: 23229486]
34. Mach KE, Mohan R, Baron EJ, Shih M-C, Gau V, Wong PK, Liao JC, A biosensor platform for rapid antimicrobial susceptibility testing directly from clinical samples. J. Urol 185, 148–153 (2011). [PubMed: 21074208]
35. Mezger A, Gullberg E, Goransson J, Zorzet A, Herthnek D, Tano E, Nilsson M, Andersson DI, A general method for rapid determination of antibiotic susceptibility and species in bacterial infections. J. Clin. Microbiol 53, 425–432 (2015). [PubMed: 25411178]
36. Rolain JM, Mallet MN, Fournier PE, Raoult D, Real-time PCR for universal antibiotic susceptibility testing. J. Antimicrob. Chemother 54, 538–541 (2004). [PubMed: 15231761]
37. Steinberger-Levy I, Shifman O, Zvi A, Ariel N, Beth-Din A, Israeli O, Gur D, Aftalion M, Maoz S, Ber R, A rapid molecular test for determining Yersinia pestis susceptibility to ciprofloxacin by the quantification of differentially expressed marker genes. Front. Microbiol 7, 763 (2016). [PubMed: 27242774]
38. Barczak AK, Gomez JE, Kaufmann BB, Hinson ER, Cosimi L, Borowsky ML, Onderdonk AB, Stanley SA, Kaur D, Bryant KF, Knipe DM, Sloutsky A, Hung DT, RNA signatures allow rapid identification of pathogens and antibiotic susceptibilities. Proc. Natl. Acad. Sci. U.S.A 109, 6217–6222 (2012). [PubMed: 22474362]
39. Fredborg M, Rosenvinge FS, Spillum E, Kroghsbo S, Wang M, Sondergaard TE, Rapid antimicrobial susceptibility testing of clinical isolates by digital time-lapse microscopy. Eur. J. Clin. Microbiol. Infect. Dis 34, 2385–2394 (2015). [PubMed: 26407621]
40. Selck DA, Karymov MA, Sun B, Ismagilov RF, Increased robustness of single-molecule counting with microfluidics, digital isothermal amplification, and a mobile phone versus real-time kinetic measurements. Anal. Chem 85, 11129–11136 (2013). [PubMed: 24199852]
41. Whale AS, Huggett JF, Cowen S, Speirs V, Shaw J, Ellison S, Foy CA, Scott DJ, Comparison of microfluidic digital PCR and conventional quantitative PCR for measuring copy number variation. Nucleic Acids Res. 40, e82 (2012). [PubMed: 22373922]

42. Haake D, Churchill B, Halford C, “Amdinocillin for rapid determination of susceptibility to beta-lactam antibiotics” (PCT/US2014/047684, international filing date 7/22/2014).
43. Almeida RJ, Jorgensen JH, Comparison of adherence and urine growth rate properties of Staphylococcus saprophyticus and Staphylococcus epidermidis. Eur. J. Clin. Microbiol 3, 542–545 (1984). [PubMed: 6526020]
44. Lawlor MS, O’Connor C, Miller VL, Yersiniabactin is a virulence factor for Klebsiella pneumoniae during pulmonary infection. Infect. Immun 75, 1463–1472 (2007). [PubMed: 17220312]
45. Kreutz JE, Munson T, Huynh T, Shen F, Du W, Ismagilov RF, Theoretical design and analysis of multivolume digital assays with wide dynamic range validated experimentally with microfluidic digital PCR. Anal. Chem 83, 8158–8168 (2011). [PubMed: 21981344]
46. Weaver S, Dube S, Mir A, Qin J, Sun G, Ramakrishnan R, Jones RC, Livak KJ, Taking qPCR to a higher level: Analysis of CNV reveals the power of high throughput qPCR to enhance quantitative resolution. Methods 50, 271–276 (2010). [PubMed: 20079846]
47. Xu P, Zheng X, Tao Y, Du W, Cross-interface emulsification for generating size-tuneable droplets. Anal. Chem 88, 3171–3177 (2016). [PubMed: 26849419]
48. Schuler F, Siber C, Hin S, Wadle S, Paust N, Zengerle R, von Stetten F, Digital droplet LAMP as a microfluidic app on standard laboratory devices. Anal. Methods 8, 2750–2755 (2016).
49. Rane TD, Chen L, Zec HC, Wang T-H, Microfluidic continuous flow digital loop-mediated isothermal amplification (LAMP). Lab Chip 15, 776–782 (2015). [PubMed: 25431886]
50. Sun B, Rodriguez-Manzano J, Selck DA, Khorosheva E, Karymov MA, Ismagilov RF, Measuring fate and rate of single-molecule competition of amplification and restriction digestion, and its use for rapid genotyping tested with hepatitis C viral RNA. Angew. Chem. Int. Ed. Engl 53, 8088–8092 (2014). [PubMed: 24889060]
51. Tanner NA, Evans TC Jr., Loop-mediated isothermal amplification for detection of nucleic acids. Curr. Protoc. Mol. Biol 105, unit 15.14 (2014).
52. Imai M, Ninomiya A, Minekawa H, Notomi T, Ishizaki T, Tashiro M, Odagiri T, Development of H5-RT-LAMP (loop-mediated isothermal amplification) system for rapid diagnosis of H5 avian influenza virus infection. Vaccine 24, 6679–6682 (2006). [PubMed: 16797110]
53. Kurosaki Y, Magassouba N, Oloniniyi OK, Cherif MS, Sakabe S, Takada A, Hirayama K, Yasuda J, Development and evaluation of reverse transcription-loop-mediated isothermal amplification (RT-LAMP) assay coupled with a portable device for rapid diagnosis of Ebola virus disease in Guinea. PLOS Negl. Trop. Dis 10, e0004472 (2016). [PubMed: 26900929]
54. Buhlmann A, Pothier JF, Rezzonico F, Smits THM, Andreou M, Boonham N, Duffy B, Frey JE, Erwinia amylovora loop-mediated isothermal amplification (LAMP) assay for rapid pathogen detection and on-site diagnosis of fire blight. J. Microbiol. Methods 92, 332–339 (2013). [PubMed: 23275135]
55. Wu GP, Chen SH, Levin RE, Application of ethidium bromide monoazide for quantification of viable and dead cells of Salmonella enterica by real-time loop-mediated isothermal amplification. J. Microbiol. Methods 117,41–48 (2015). [PubMed: 26187777]
56. Selck DA, Ismagilov RF, Instrument for real-time digital nucleic acid amplification on custom microfluidic devices. PLOS ONE 11 , e0163060 (2016). [PubMed: 27760148]
57. Shen F, Du W, Kreutz JE, Fok A, Ismagilov RF, Digital PCR on a SlipChip. Lab Chip 10, 2666–2672 (2010). [PubMed: 20596567]
58. Gillespie DT, Stochastic simulation of chemical kinetics. Annu. Rev. Phys. Chem 58, 35–55 (2007). [PubMed: 17037977]
59. Clinical and Laboratory Standards Institute (CLSI), Performance standards for antimicrobial susceptibility testing (M100–S25, CLSI, 2015).
60. Turnidge J, Paterson DL, Setting and revising antibacterial susceptibility breakpoints. Clin. Microbiol. Rev 20, 391–408 (2007). [PubMed: 17630331]
61. Ivancic V, Mastali M, Percy N, Gornbein J, Babbitt JT, Li Y, Landaw EM, Bruckner DA, Churchill BM, Haake DA, Rapid antimicrobial susceptibility determination of uropathogens in clinical urine specimens by use of ATP bioluminescence. J. Clin. Microbiol 46, 1213–1219 (2008). [PubMed: 18272708]

62. European Committee on Antimicrobial Susceptibility Testing (EUCAST), Antimicrobial wild type distributions of microorganisms (EUCAST, 2017); https://mic.eucast.org/Eucast2/.
63. Shen F, Davydova EK, Du W, Kreutz JE, Piepenburg O, Ismagilov RF, Digital isothermal quantification of nucleic acids via simultaneous chemical initiation of recombinase polymerase amplification reactions on SlipChip. Anal. Chem 83, 3533–3540 (2011). [PubMed: 21476587]
64. Sun B, Shen F, McCalla SE, Kreutz JE, Karymov MA, Ismagilov RF, Mechanistic evaluation of the pros and cons of digital RT-LAMP for HIV-1 viral load quantification on a microfluidic device and improved efficiency via a two-step digital protocol. Anal. Chem 85, 1540–1546 (2013). [PubMed: 23324061]
65. Notomi T, Mori Y, Tomita N, Kanda H, Loop-mediated isothermal amplification (LAMP): Principle, features, and future prospects. J. Microbiol 53, 1–5 (2015). [PubMed: 25557475]
66. Tanner NA, Evans TC, "Compositions and Methods for Reducing Background DNA Amplification" (US20130323793, filing date 3/13/2013).
67. Martin A, Grant KB, Stressmann F, Ghigo J-M, Marchal D, Limoges B, Ultimate single-copy DNA detection using real-time electrochemical LAMP. ACS Sens 1, 904–912 (2016).
68. Tanner NA, Zhang Y, Evans TC Jr., Simultaneous m ultiple target detection in real-time loop-mediated isothermal amplification. Biotechniques 53, 81–89 (2012). [PubMed: 23030060]
69. Tanner NA, Zhang Y, Evans TC Jr., Visual detection of isothermal nucleic acid amplification using pH-sensitive dyes. Biotechniques 58, 59–68 (2015). [PubMed: 25652028]
70. Rodriguez-Manzano J, Karymov MA, Begolo S, Selck DA, Zhukov DV, Jue E, Ismagilov RF, Reading out single-molecule digital RNA and DNA isothermal amplification in nanoliter volumes with unmodified camera phones. ACS Nano 10, 3102–3113 (2016). [PubMed: 26900709]
71. Simerville JA, Maxted WC, Pahira JJ, Urinalysis: A comprehensive review. Am. Fam. Physician 71, 1153–1162 (2005). [PubMed: 15791892]
72. Courbet A, Endy D, Renard E, Molina F, Bonnet J, Detection of pathological biomarkers in human clinical samples via amplifying genetic switches and logic gates. Sci. Transl. Med 7, 289ra83 (2015).
73. Laksanasopin T, Guo TW, Nayak S, Sridhara AA, Xie S, Olowookere OO, Cadinu P, Meng F, Chee NH, Kim J, Chin CD, Munyazesa E, Mugwaneza P, Mugisha AJV, Castro AR, Steinmiller D, Linder V, Justman JE, Nsanzimana S, Sia SK, A smartphone dongle for diagnosis of infectious diseases at the point of care. Sci. Transl. Med 7, 273re1 (2015).
74. Watkins NN, Hassan U, Damhorst G, Ni H, Vaid A, Rodriguez W, Bashir R, Microfluidic CD4+ and CD8+ T lymphocyte counters for point-of-care HIV diagnostics using whole blood. Sci. Transl. Med 5, 214ra170 (2013).
75. Kallen AJ, Welch HG, Sirovich BE, Current antibiotic therapy for isolated urinary tract infections in women. Arch. Intern. Med 166, 635–639 (2006). [PubMed: 16567602]
76. Shen F, Sun B, Kreutz JE, Davydova EK, Du W, Reddy PL, Joseph LJ, Ismagilov RF, Multiplexed quantification of nucleic acids with large dynamic range using multivolume digital RT-PCR on a rotational SlipChip tested with HIV and hepatitis C viral load. J. Am. Chem. Soc 133, 17705–17712 (2011). [PubMed: 21995644]
77. Walsh AL, Smith MD, Wuthiekanun V, Suputtamongkol Y, Chaowagul W, Dance DAB, Angus B, White NJ, Prognostic significance of quantitative bacteremia in septicemic melioidosis. Clin. Infect. Dis 21, 1498–1500 (1995). [PubMed: 8749644]
78. Musta AC, Riederer K, Shemes S, Chase P, Jose J, Johnson LB, Khatib R, Vancomycin MIC plus heteroresistance and outcome of methicillin-resistant Staphylococcus aureus bacteremia: Trends over 11 years. J. Clin. Microbiol 47, 1640–1644 (2009). [PubMed: 19369444]
79. Schuler F, Schwemmer F, Trotter M, Wadle S, Zengerle R, von Stetten F, Paust N, Centrifugal step emulsification applied for absolute quantification of nucleic acids by digital droplet RPA. Lab Chip 15, 2759–2766 (2015). [PubMed: 25947077]
80. Witters D, Sun B, Begolo S, Rodriguez-Manzano J, Robles W, Ismagilov RF, Digital biology and chemistry. Lab Chip 14, 3225–3232 (2014). [PubMed: 24889331]
81. Hayashida K, Kajino K, Hachaambwa L, Namangala B, Sugimoto C, Direct blood dry LAMP: A rapid, stable, and easy diagnostic tool for Human African Trypanosomiasis. PLOS Negl. Trop. Dis 9, e0003578 (2015). [PubMed: 25769046]

82. Jevtusevskaja J, Krolov K, Tulp I, Langel U, The effect of main urine inhibitors on the activity of different DNA polymerases in loop-mediated isothermal amplification. Expert Rev. Mol. Diagn 17, 403–410 (2017).
83. Dingle TC, Sedlak RH, Cook L, Jerome KR, Tolerance of droplet-digital PCR vs real-time quantitative PCR to inhibitory substances. Clin. Chem 59, 1670–1672 (2013). [PubMed: 24003063]
84. Sedlak RH, Kuypers J, Jerome KR, A multiplexed droplet digital PCR assay performs better than qPCR on inhibition prone samples. Diagn. Microbiol. Infect. Dis 80, 285–286 (2014). [PubMed: 25277746]
85. Whale AS, Devonshire AS, Karlin-Neumann G, Regan J, Javier L, Cowen S, Fernandez-Gonzalez A, Jones GM, Redshaw N, Beck J, Berger AW, Combaret V, Dahl Kjersgaard N, Davis L, Fina F, Forshew T, Fredslund Andersen R, Galbiati S, Gonzalez Hernandez A, Haynes CA, Janku F, Lacave R, Lee J, Mistry V, Pender A, Pradines A, Proudhon C, Saal LH, Stieglitz E, Ulrich B, Foy CA, Parkes H, Tzonev S, Huggett JF, International interlaboratory digital PCR study demonstrating high reproducibility for the measurement of a rare sequence variant. Anal. Chem 89, 1724–1733 (2017). [PubMed: 27935690]
86. Banoo S, Bell D, Bossuyt P, Herring A, Mabey D, Poole F, Smith PG, Sriram N, Wongsrichanalai C, Linke R, O'Brien R, Perkins M, Cunningham J, Matsoso P, Nathanson CM, Olliaro P, Peeling RW, Ramsay A; TDR Diagnostics Evaluation Expert Panel, Evaluation of diagnostic tests for infectious diseases: General principles. Nat. Rev. Microbiol 4, S21–S31 (2006). [PubMed: 17034069]
87. Ku HH, Notes on the use of propagation of error formulas. J. Res. Natl. Bur. Stand. Sect C 70C, 263–273 (1966).
88. Stenholm T, Hakanen AJ, Hakanen E, Harma H, Osterblad M, Vuopio J, Hanninen PE, Huovinen P, Rankakokko-Jalava K, Kotilainen P, High-throughput screening of colonization samples for methicillin-resistant Staphylococcus aureus. Scand. J. Infect. Dis 45, 922–929 (2013).
89. Lu Y, Gao J, Zhang DD, Gau V, Liao JC, Wong PK, Single cell antimicrobial susceptibility testing by confined microchannels and electrokinetic loading. Anal. Chem 85, 3971–3976 (2013). [PubMed: 23445209]
90. Besant JD, Sargent EH, Kelley SO, Rapid electrochemical phenotypic profiling of antibiotic-resistant bacteria. Lab Chip 15, 2799–2807 (2015). [PubMed: 26008802]
91. Chen CH, Lu Y, Sin MLY, Mach KE, Zhang DD, Gau V, Liao JC, Wong PK, Antimicrobial susceptibility testing using high surface-to-volume ratio microchannels. Anal. Chem 82, 1012–1019 (2010). [PubMed: 20055494]
92. Broeren MAC, Maas Y, Retera E, Arents NLA, Antimicrobial susceptibility testing in 90 min bybacterial cell count monitoring.Clin. Microbiol. Infect 19,286–291 (2013). [PubMed: 22390723]
93. Sinn I, Kinnunen P, Albertson T, McNaughton BH, Newton DW, Burns MA, Kopelman R, Asynchronous magnetic bead rotation (AMBR) biosensor in microfluidic droplets for rapid bacterial growth and susceptibility measurements. Lab Chip 11, 2604–2611 (2011). [PubMed: 21666890]
94. Liu C-Y, Han Y-Y, Shih P-H, Lian W-N, Wang H-H, Lin C-H, Hsueh P-R, Wang J-K, Wang Y-L, Rapid bacterial antibiotic susceptibility test based on simple surface-enhanced Raman spectroscopic biomarkers. Sci. Rep 6, 23375 (2016). [PubMed: 26997474]
95. Liu T-T, Lin Y-H, Hung C-S, Liu T-J, Chen Y, Huang Y-C, Tsai T-H, Wang H-H, Wang D-W, Wang J-K, Wang Y-L, Lin C-H, A high speed detection platform based on surface-enhanced Raman scattering for monitoring antibiotic-induced chemical changes in bacteria cell wall. PLOS ONE 4, e5470 (2009). [PubMed: 19421405]
96. Shrestha NK, Scalera NM, Wilson DA, Procop GW, Rapid differentiation of methicillin-resistant and methicillin-susceptible Staphylococcus aureus by flow cytometry after brief antibiotic exposure. J. Clin. Microbiol 49, 2116–2120 (2011). [PubMed: 21471343]
97. Faria-Ramos I, Espinar MJ, Rocha R, Santos-Antunes J, Rodrigues AG, Cantón R, Pina-Vaz C, A novel flow cytometric assay for rapid detection of extended-spectrum beta-lactamases. Clin. Microbiol. Infect 19, E8–E15 (2013). [PubMed: 23145853]

98. Lange C, Schubert S, Jung J, Kostrzewa M, Sparbier K, Quantitative matrix-assisted laser desorption ionization-time of flight mass spectrometry for rapid resistance detection. J. Clin. Microbiol 52, 4155–4162 (2014). [PubMed: 25232164]

99. Mann TS, Mikkelsen SR, Antibiotic susceptibility testing at a screen-printed carbon electrode array. Anal. Chem 80, 843–848 (2008). [PubMed: 18181646]

100. Tang Y, Zhen L, Liu J, Wu J, Rapid antibiotic susceptibility testing in a microfluidic pH sensor. Anal. Chem 85, 2787–2794 (2013). [PubMed: 23360389]

101. Roth BL, Poot M, Yue ST, Millard PJ, Bacterial viability and antibiotic susceptibility testing with SYTOX green nucleic acid stain. Appl. Environ. Microbiol 63, 2421–2431 (1997). [PubMed: 9172364]

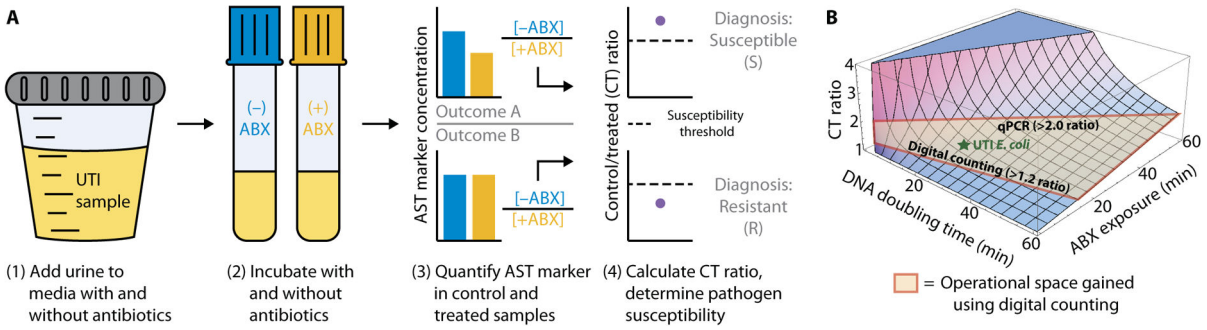

Fig. 1. Experimental workflow of the dAST method and computationally estimated operational space.

(**A**) The workflow for detecting antibiotic susceptibility by measuring the quantity of a specific NA sequence (AST marker). Urine samples are incubated without and with antibiotics (ABX) (steps 1 and 2), AST markers are quantified in control (−ABX) and treated (+ABX) samples (step 3), and the CT ratios are analyzed (step 4). (**B**) Theoretical model that predicts a CT ratio as a function of pathogen DNA doubling time and antibiotic exposure time. The operational space gained by using digital counting compared with qPCR is outlined in red.

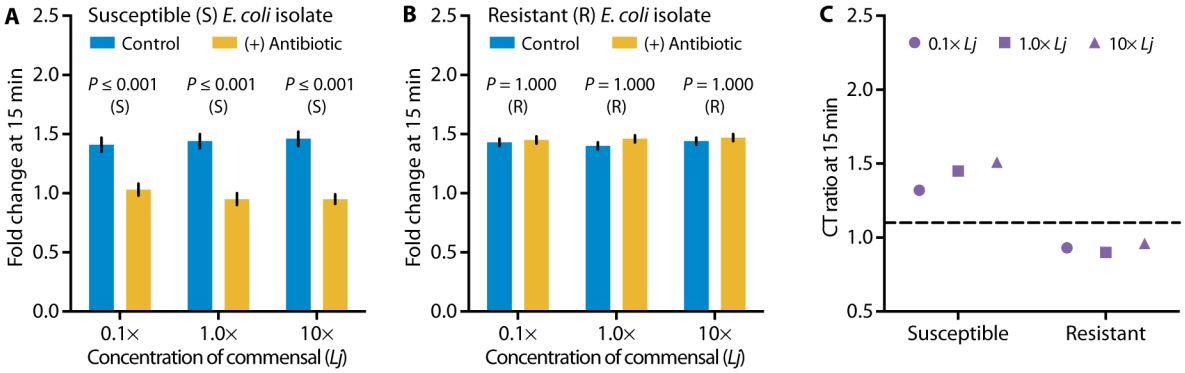

Fig. 2. dAST using dPCR is robust to the presence of high concentrations of commensal bacteria due to the specificity of NA amplification.

(**A**) A cip-susceptible *E. coli* isolate and (**B**) a cip-resistant *E. coli* isolate from the urine of patients diagnosed with UTIs were exposed to cip (1.0 μg/ml) in the presence of varying amounts of *Lj*, a common urine commensal. Fold changes relative to time 0 were compared as described in (26) and used to determine susceptibility. (**C**) Susceptibility determined using the CT ratios after 15 min of antibiotic exposure for each concentration of Lj tested. *n* = 2 technical replicates for each biological sample. Error bars are 98% confidence intervals.

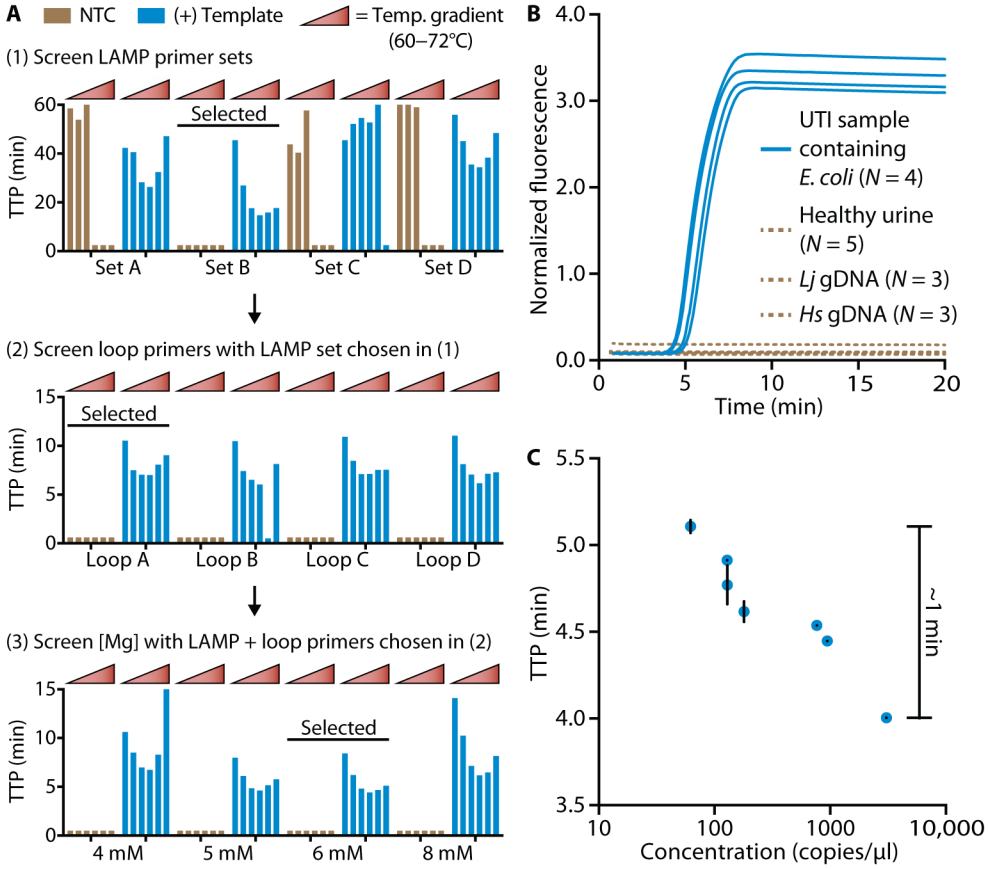

Fig. 3. Real-time LAMP optimization and compatibility with clinical samples.

(**A**) Assay optimization protocol used to reduce the TTP from 15 to <5 min. Optimization was performed at a template concentration of ~700 or 0 copies per reaction. NTC, no template control. A value of 0.5 indicates that no amplification was observed. $n = 1$ for all TTP values. (**B**) Real-time fluorescence readout of amplified DNA for UTI urine samples containing *E. coli* (blue lines), healthy urine samples, urine samples containing gDNA of *Lj*, and urine samples containing human (*Hs*) gDNA (dashed brown lines). (**C**) TTP values for clinical UTI urine samples containing a range of pathogen concentrations. Error bars represent a single SD from the average of technical triplicates. $n = 3$ technical replicates for each TTP value.

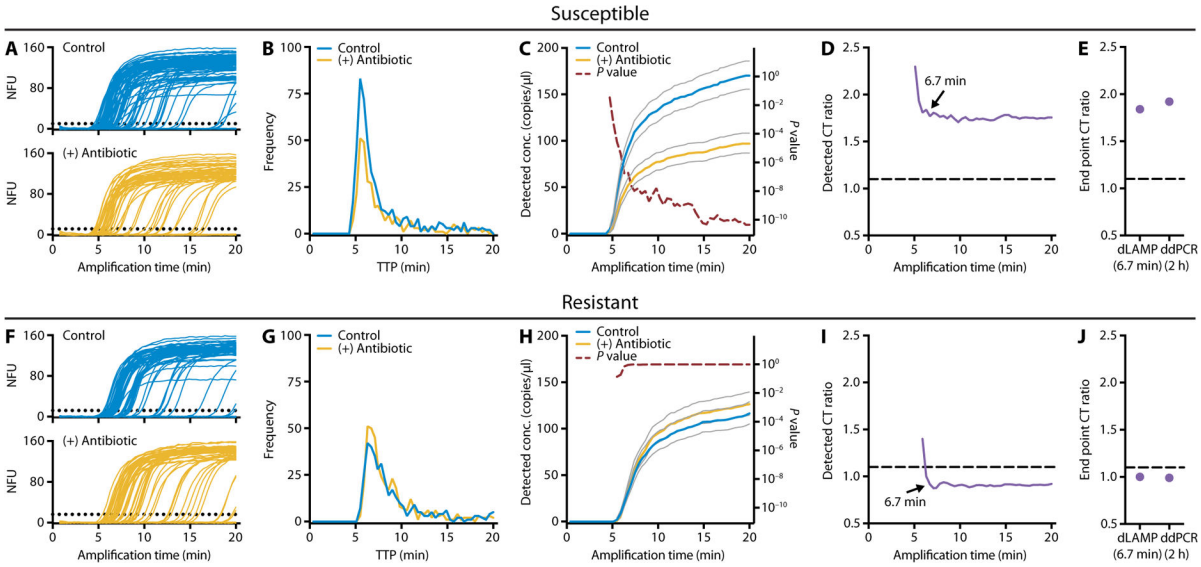

Fig. 4. High-resolution single-molecule NA amplification using ultrafast dLAMP for dAST of clinical UTI urine samples.

UTI urine samples with (**A** to **E**) antibiotic-susceptible and (**F** to **J**) antibiotic-resistant *E. coli*. (A and F) Real-time fluorescence amplification traces (200 of 1280 traces shown for clarity). NFU, normalized fluorescence units; dotted line, positive threshold. When the normalized fluorescence intensity of a compartment crosses the threshold, that compartment is counted as positive. (B and G) TTP distribution determined by counting the number of compartments that crossed the positive threshold at each time point. (C and H) Detected concentrations of the target dAST marker in control and antibiotic-treated samples for successive image cycles. Note that these curves are distinct from the amplification curves shown in (A) and (F). Gray lines represent 95% confidence intervals. *P* values were calculated using a *Z* test (see Statistical analysis). (D and I) Detected CT ratios over time. Dashed line indicates susceptibility threshold. (E and J) Comparison of the CT ratios for droplet digital PCR (ddPCR) after 2 hours and dLAMP after 6.7 min of amplification.

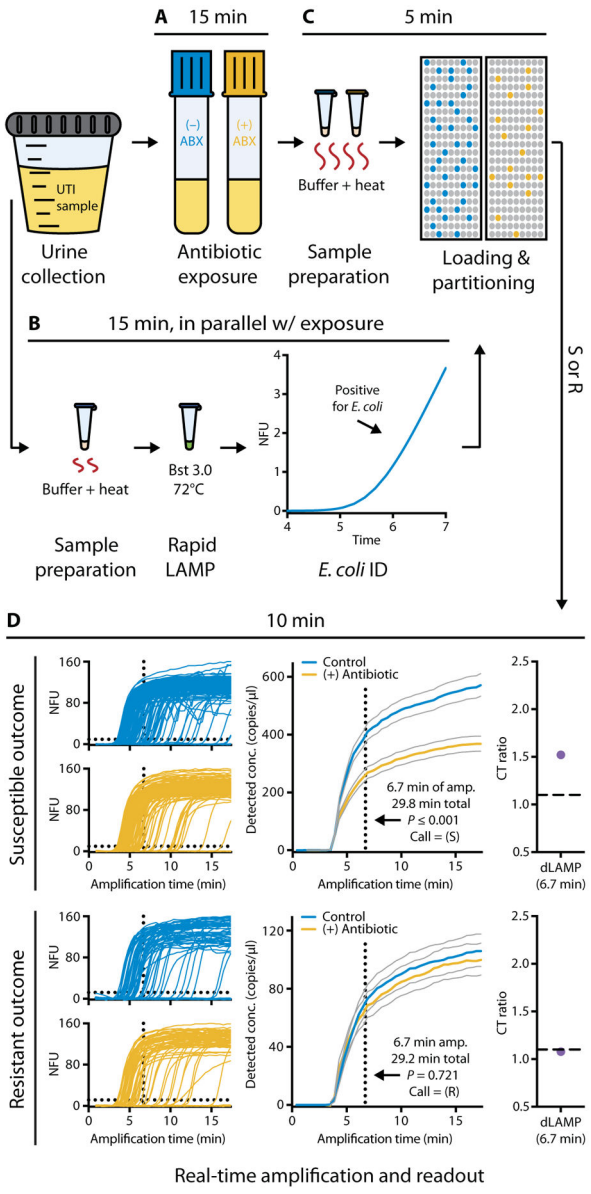

Fig. 5. Workflow of a sample-to-answer AST performed in less than 30 min.

(**A**) A clinical UTI sample was added to media with and without cip and incubated for 15 min. (**B**) During the antibiotic exposure step, the optimized bulk LAMP assay was performed on NAs prepared from an aliquot of the urine sample. Amplification indicated the presence of *E. coli* at clinically relevant concentrations. (**C**) Aliquots of the control and antibiotic-treated samples were added to extraction buffer, NAs were prepared for quantification using dLAMP, and samples were rapidly partitioned using SlipChips. (**D**) dLAMP was monitored in real time, and a susceptibility call was determined after 6.7 min of amplification; data for one resistant and one susceptible sample are shown. *P* values were calculated using a *Z* test (see Statistical analysis). Gray lines represent 95% confidence intervals.

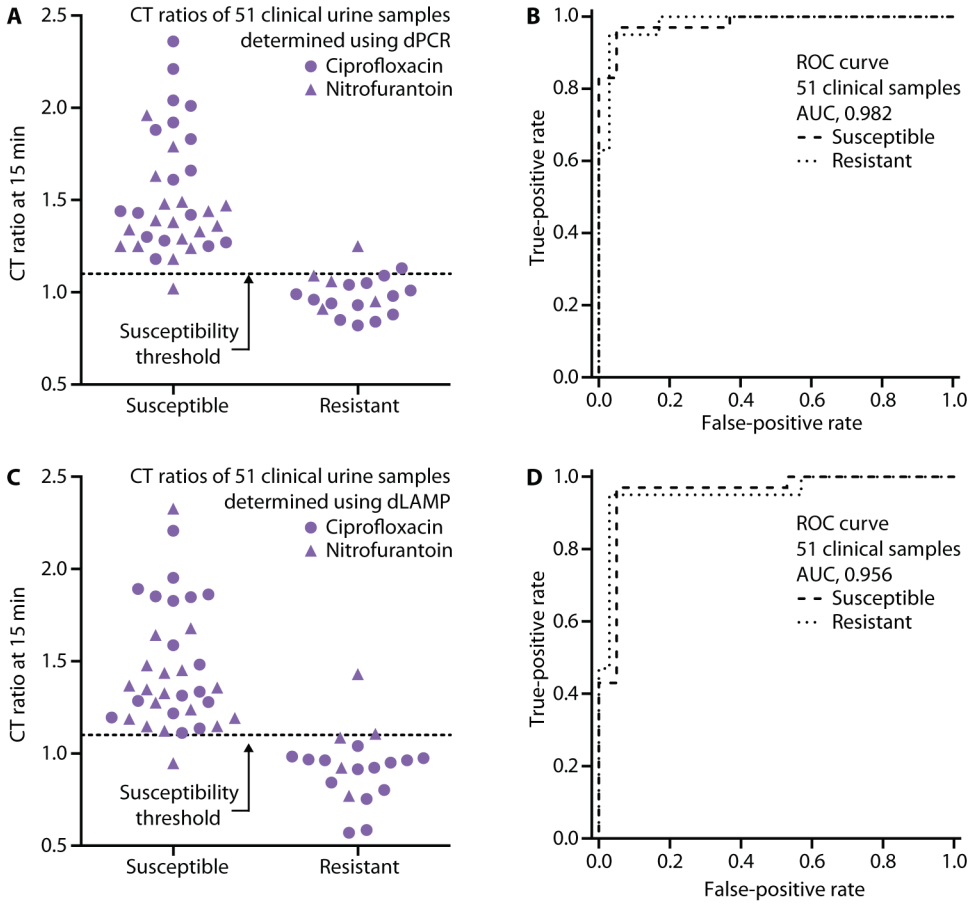

Fig. 6. dAST directly from clinical samples using dPCRand dLAMPfor quantification.

(**A** and **C**) Antibiotic susceptibility of 51 clinical *E. coli*–infected UTI samples determined using the CT ratios after 15 min of exposure to nit and cip (35 susceptible and 19 resistant; 3 samples were tested for both antibiotics). NA concentrations were quantified with dPCR (A) and dLAMP (C). (**B** and **D**) ROC curves for the dAST method as measured by dPCR (B) and dLAMP (D).